Surface and interface states for GaAs(100) (1×1) and (4×2)-c(8×2) reconstructions

I. M. Vitomirov, A. D. Raisanen, A. C. Finnefrock, R. E. Viturro, S. Chang, and L. J. Brillson
Xerox Webster Research Center, Webster, New York 14580

P. D. Kirchner, G. D. Pettit, and J. M. Woodall
IBM T. J. Watson Research Center, Yorktown Heights, New York 10598

(Received 9 December 1991; accepted 2 March 1992)

Low energy cathodoluminescence spectroscopy measurements of GaAs(100) surfaces prepared by thermal desorption of an As passivation layer reveal deep level transitions localized at the clean surfaces and metallized interfaces. These surface and interface state features extend from 0.7 to 1.3 eV and exhibit subtle differences between the As-rich (1×1) and Ga-rich (4×2)-c(8×2) reconstructions. Both Au deposition and subsequent annealing induce additional deep level emissions which appear relatively unchanged between these two reconstructions. In contrast, Al deposition introduces new features which depend significantly upon starting surface stoichiometry and reconstruction. We discuss the formation and energies of these states in relation to reported variations in Fermi level stabilization. We conclude that surface stoichiometry and atomic bond configuration are a significant factor in formation and evolution of electrically active, deep level metal-GaAs(100) interface states.

I. INTRODUCTION

The relationship between surface atomic structure and electronic properties has been a focus of much research on metal–semiconductor interfaces.[1–5] The GaAs(100) surfaces and their interfaces with metals have attracted particular interest for several reasons: (i) This surface gives rise to a multiplicity of surface reconstructions which depend sensitively on conditions of growth and annealing.[6–11] (ii) These reconstructions span a wide range of surface stoichiometry and atomic bond configurations. (iii) Metals on the GaAs(100) surface exhibit qualitative differences in Fermi level (E_F) evolution and barrier formation versus GaAs(110) cleavage surfaces.[12,13] (iv) There is as yet no consensus for the barrier heights reported for metals on GaAs(100). Viturro *et al.*[12,13] have reported a wide range of barriers exhibiting near-ideal behavior whereas Mao *et al.*,[14] Spindt *et al.*,[15] and Wilks *et al.*[16] have reported substantially lower barrier variation for metals on GaAs(100). These differences may in part be related to variations in surface preparation, surface photovoltage effects,[17] and artifacts in the data analysis.[18]

Here we report observations of deep level electronic states associated with two reconstructions of the GaAs(100) surface. The (1×1) and (4×2)-c(8×2) reconstructions reported here provide a comparison of surface electronic states associated with a strongly As-rich versus Ga-rich surface. In addition, we have monitored the changes in such states upon metal deposition using both Au and Al metals with significantly different interface chemistry.[4,5] Comparison of the interface states induced by these metals provides a gauge of the relative importance of low-energy electron diffraction (LEED) reconstruction, surface stoichiometry, and interface reaction/diffusion on the interface deep level features. Our results indicate: (a) subtle differences in deep level emission for these two clean surface reconstructions, (b) significant changes in discrete deep level features with metallization, (c) qualitatively different effects for the two metals. In particular, we observe Au-induced features which are relatively independent of reconstruction, Al-induced features which differ significantly between the two reconstructions, and increased differences in interface features with annealing of the two Al/GaAs(100) reconstruction interfaces. On this basis, we conclude that surface stoichiometry and atomic bond configuration are a significant factor in formation and evolution of deep level metal-GaAs(100) interface states.

II. EXPERIMENTAL DESCRIPTION

We performed low energy cathodoluminescence spectroscopy (CLS) and photoluminescence spectroscopy (PL) measurements of the GaAs surface and interfaces in an ultrahigh vacuum (UHV) chamber (base pressure 1×10^{-10} Torr) equipped with a >1000 l/s cryopump. The low energy CLS technique[19,20] involves excitation by a chopped electron beam (1–10 A cm^{-2}) from a 1–2 kV glancing incidence electron gun. In CLS photodetection, the luminescence signal travels from the excited specimen through a single-pass Leiss prism monochromator employing IR and visible optics into a liquid-nitrogen-cooled Ge photodiode with phase detection via a lock-in amplifier. The variable energy of excitation facilitates identification of interface specific versus bulk features since excitation depth and maximum steady state excess carrier concentrations at the near-surface region are strongly energy dependent within this energy range.[19,20] PL excitation consisted of a HeNe laser (6 mW at 1.96 eV). CLS and PL spectra were deconvolved by comparison with a black body spectrum associated with the measured spectrum of a W filament with known temperature. The GaAs(100) surfaces (Si doped, $n=7–10\times10^{16}$ cm^{-3} were grown by

 0734-2101/92/040749-05$01.00

molecular-beam epitaxy (MBE), passivated by a thick (~ 5000 Å) As layer, and shipped under N_2 overpressure in a stainless steel vessel from Yorktown Heights to Webster, NY and thermally decapped in the UHV chamber. Typical ramp heating rates were 2–10 °C s^{-1}. We obtained different reconstructions by annealing the GaAs(100) surface to a given temperature for ~ 5 min. Surface temperatures were monitored by an Optitherm Radiometer focused on the front GaAs face. A reverse-view, low-energy electron diffraction (LEED) screen provided a visual indicator of the temperature-dependent reconstruction following the thermal treatments. A closed-cycle He refrigerator provided specimen cooling to 180 K during CLS and PL measurements. Ta spring clips with Au-foil contacts held against the GaAs(100) front face anchored the specimens and provided low resistance current pathways to ground. Metal deposition involved evaporation from preoutgassed W baskets on to the thermally annealed GaAs(100) surfaces and to a quartz crystal oscillator thickness monitor positioned nearby. Deposition rates were typically 1 Å/min. We used soft x-ray photoemission spectroscopy (SXPS) and Auger electron spectroscopy to monitor surface Ga/As stoichiometry and chemical contamination. After desorption, Auger measurements showed no detectable presence of C and O contamination. A minicomputer provided control of monochromator scan energies, data acquisition, and thermal annealing.

III. DEEP LEVEL EMISSION SPECTRA OF CLEAN GaAs(100) SURFACES

We have measured CL spectra for three clean GaAs(100) surfaces: (a) a (1×1) reconstruction obtained with a 350 °C anneal of GaAs(100) ($n = 7\times10^{16}$ cm^{-3}), (b) a (4×2)-$c(8\times2)$ reconstruction obtained with a 575 °C anneal of GaAs(100) ($n = 7\times10^{16}$ cm^{-3}), and (c) a (4×2)-$c(8\times2)$ reconstruction obtained with a 520 °C anneal of GaAs(100) ($n = 1\times10^{17}$ cm^{-3}). Respective stoichiometries for these reconstructed surfaces are: (a) 1.5, (b) 0.9, and (c) 1.0, as derived from the ratio of the total As 3*d* and Ga 3*d* core level emission intensities measured at $h\nu = 100$ and 80 eV, respectively. Figure 1 displays CLS spectral features for excitation energies of 1, 1.5, and 2 keV for both the 575 and 350 °C anneals. Figure 1(a) illustrates dominant near band gap (NBG) emission at 1.47 eV. This energy defines the temperature-dependent band gap of the specimen.[21] Also shown are a set of deep level emission features which extend from below 0.8 eV to ~ 1.3 eV. With decreasing excitation energy these features increase in spectral intensity and exhibit a maximum at 1.2–1.25 eV. While the detailed spectral distribution depends upon the specific thermal processing, the peak intensity increase with decreasing excitation energy is consistent with discrete deep levels localized near the semiconductor surface.[19,20] Figure 1(b) shows the analogous CLS spectral features for the same excitation energies on a lower temperature reconstruction of the same ($n = 7\times10^{16}$ cm^{-3}) GaAs(100) material. Here the spectral intensity of deep level emission is relatively insensitive to the excitation energy and corresponding probe depth. The weak energy dependence of these features is consistent either with deep level features which extend tens of nanometers below the surface or a very narrow (~ 100 Å) depletion region with relatively low free carrier migration toward and recombination at the surface. The latter is not likely due to the relatively low bulk carrier concentration.

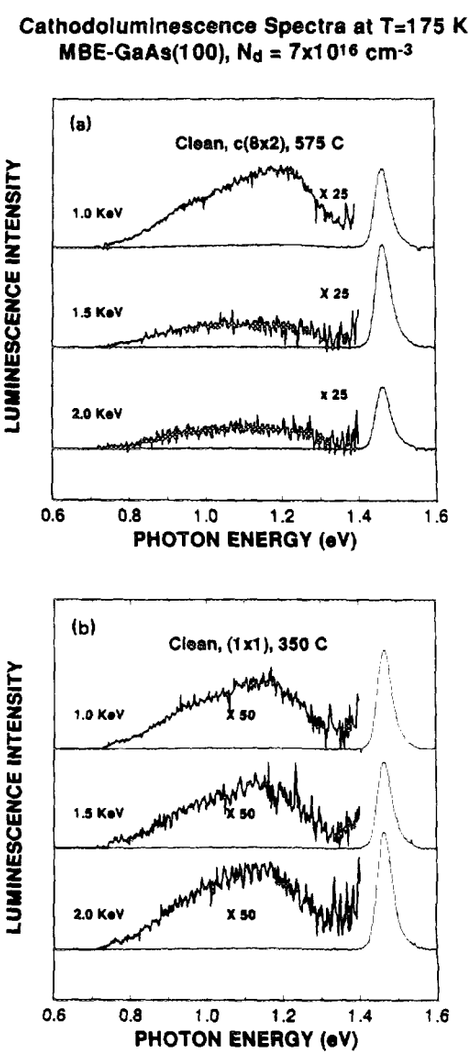

FIG. 1. Low energy cathodoluminescence spectra taken at 175 K of MBE-grown GaAs(100) surfaces at three excitation voltages for (a) a (4×2)-$c(8\times2)$ prepared at 575 °C and (b) a (1×1) reconstruction prepared at 350 °C. With decreasing excitation voltage in (a), emission intensity below the 1.47 eV near band edge peak increases, consistent with the near-surface nature of the deep level feature. Different spectral line shape features appear in (b) which are relatively insensitive to excitation voltage, indicative of deep level features which extend beyond the surface.

Comparison of Figs. 1(a) and 1(b) reveals subtle but significant differences between the (1×1) and $c(8\times2)$ surfaces. Figure 2 represents the most surface sensitive (e.g., 1 kV) CLS spectra for the two reconstructions in Fig. 1[(a) and (b), respectively]. When normalized to the same maximum deep level emission intensity, curves (a) and (b) yield the difference spectrum [(a)–(b)]. The latter exhibits enhanced emission in the 0.7–1.1 eV energy range

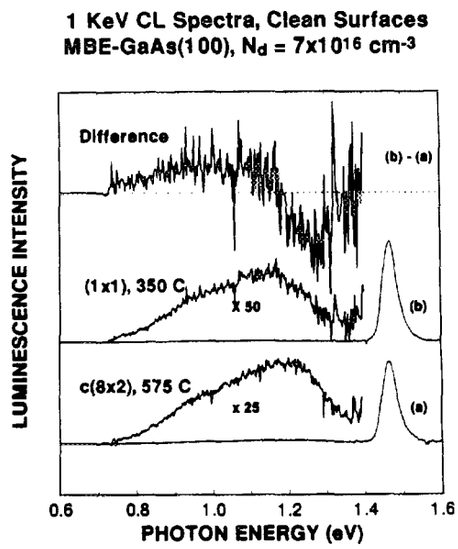

FIG. 2. Comparison of surface-sensitive CLS features for (a) the (4×2)-c-(8×2) vs (b) the (1×1) reconstructured surfaces shown in Fig. 1. The difference spectrum (b)–(a) illustrates the additional emission present in the range 0.7–1.2 eV for the (1×1) GaAs(100) surface and the additional emission present in the 1.2–1.4 eV range for the (4×2)-$c(8\times2)$ reconstructed surface.

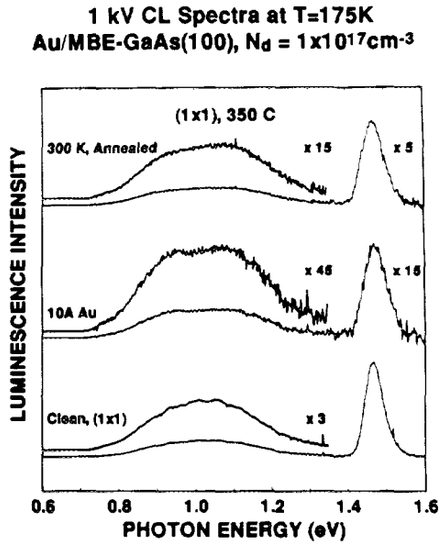

FIG. 3. Low energy cathodoluminescence spectra taken at 175 K of MBE-grown GaAs(100) surfaces at 1 kV excitation voltage for the GaAs(100) (1×1) surface prepared at 350 °C, coated with 10 Å Au, and annealed at 300 K. Au deposition induces additional emission at ~0.9 and 1.1 eV, which is further enhanced by annealing. Similar features are evident for Au on the (4×2)-$c(8\times2)$ surface.

and reduced emission from 1.2 to 1.4 eV. While the deep level CLS emission can vary among $c(8\times2)$ surfaces prepared at different temperatures, the relative change in intensities of these two energy ranges appears to be a characteristic difference between the two reconstructed surfaces.

IV. DEEP LEVEL EMISSION SPECTRA OF Au ON GaAs(100) RECONSTRUCTED SURFACES

Metal deposition on GaAs(100) surfaces induces new deep level emission features. In turn, these metal-induced optical transitions exhibit pronounced features whose dependence on reconstruction varies with metal. Figure 3 illustrates surface-sensitive CLS spectra for the clean (1×1) GaAs(100) surface after initial preparation, deposition of 10 Å Au, and subsequent annealing at 300 K. Both metallization and annealing increase the deep level emission relative to the NBG peak emission. The 10 Å Au spectrum contains additional emissions with maximum intensities at 0.92 and 1.17 eV. The 300 K annealed spectrum contains enhanced emission with maximum intensities at 1.17 and 1.05 eV. Similar comparisons at higher excitation energies (e.g., 1.5 and 2 kV) exhibit little or no changes. Hence, Au deposition and annealing both contribute to new deep level emission features associated with states localized near the metal–semiconductor interface. Furthermore, metallization with 10 Å Au and annealing at 300 K of a $c(8\times2)$ reconstructured surface lead to surface-sensitive CLS features which are essentially unchanged from those of the metallized and annealed (1×1) surface. Therefore, interface states associated with Au metallization appear to be relatively insensitive to surface stoichiometry and/or bond configuration.

V. DEEP LEVEL EMISSION SPECTRA OF Al ON GaAs(100) RECONSTRUCTED SURFACES

Deposition of Al on GaAs(100) induces new CLS spectral features which depend upon the clean surface reconstruction and stoichiometry. Figure 4 illustrates the spectral emission measured for Al on the (4×2)-$c(8\times2)$ versus the (1×1) GaAs(100) surfaces. In Fig. 4(a), deposition of 10 Å Al on the clean (4×2)-$c(8\times2)$ surface prepared at 575 °C produces new deep level emission in the range from 0.8 to 1.1 eV. The difference spectrum indicates a dominant peak located at 0.95–1.0 eV with an additional shoulder at ~0.8 eV. This is represented as the upper curve in Fig. 5. Subsequent annealing of the metallized surface at 410 °C eliminates these metal-induced emission features. A difference spectrum of the metallized and annealed versus the clean surface exhibits negligible differences in the energy range below 1.1 eV, but it indicates the presence of a new emission feature at ~1.33 eV. The energy of this feature suggests that it might be associated with an As vacancy-Si complex, possibly induced by the Al–As interfacial reaction promoted by the 410 °C anneal.[22,23] Such As vacancies (V_{As}) can also be induced by excessive heating during the initial As desorption from the clean surface, in which case the appearance of the 1.33 eV emission in the topmost spectrum (but not the other two) would be due to an accidental contribution from an overheated edge area of the sample.[24] The latter possibility is corroborated by the relative enhancement of the 1.33 eV

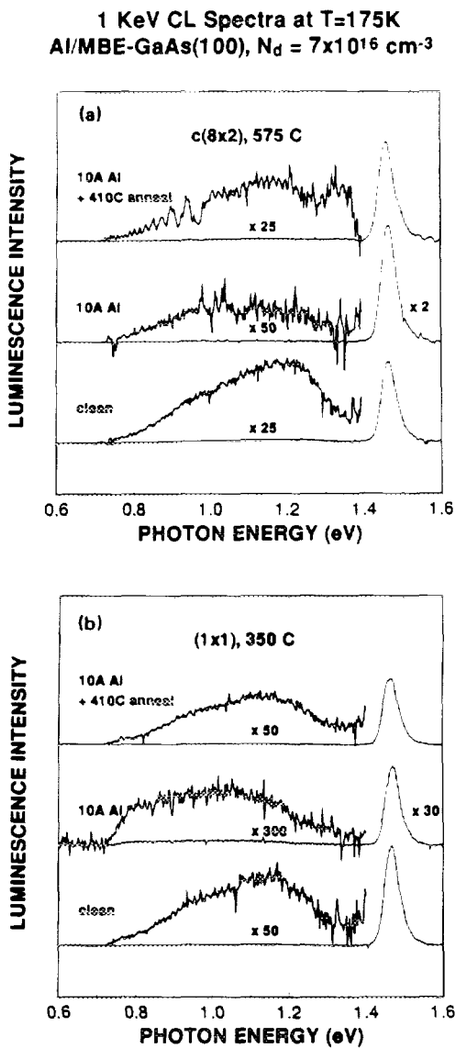

FIG. 4. Low energy cathodoluminescence spectra taken at 175 K of MBE-grown GaAs(100) surfaces at 1 kV excitation voltage for: (a) the GaAs(100) (4×2)-$c(8\times2)$ surface prepared at 575 °C, coated with 10 Å Al, and annealed for 5 min at 410 °C; (b) the GaAs(100) (1×1) surface prepared at 350 °C, coated with 10 Å Al, and annealed for 5 min at 410 °C. Al deposition induces additional emission at $\leq$0.8 and 0.95–1.0 eV, which is removed by annealing in both cases. Furthermore, the metal-induced emission exhibits different spectral distributions for the two reconstructions.

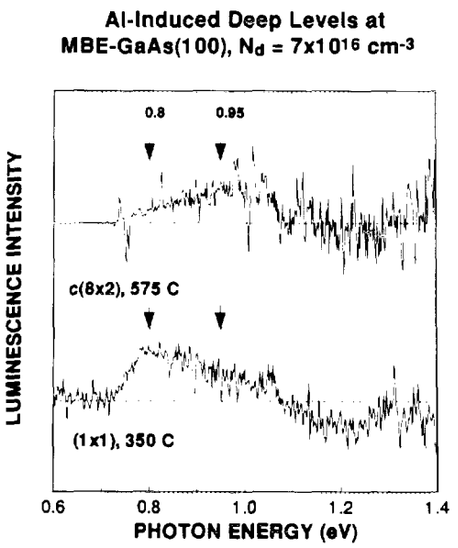

FIG. 5. Comparison of surface-sensitive CLS difference spectra from Fig. 4 for (upper) the (4×2)-$c(8\times2)$ with and without 10 Å Al and (lower) the (1×1) reconstructed surface also with and without 10 Å Al. The 0.95–1.0 eV feature dominates the deep level emission for the (4×2)-$c(8\times2)$ surface while the $\leq$0.8 feature dominates for the (1×1) reconstruction.

emission for more bulk-sensitive spectra, indicative of the subsurface location of As vacancies.

The analogous processing of the (1×1) surface also induces new deep level emission, as shown in Fig. 4(b). However, the dominant emission appears shifted to lower energies. Indeed a difference spectrum of the metallized versus the clean surface exhibits a dominant emission feature at 0.8 eV and a secondary peak centered at $\sim$0.95 eV. This is pictured as the lower curve in Fig. 5. Comparison of the two Al/GaAs(100) spectra in Fig. 5 indicate substantial differences in the relative intensities of 0.8 versus 0.95–1.0 eV emissions. Subsequent annealing of the metallized (1×1) surface at 410 °C in Fig. 4(b) eliminates the metal-induced emission features as in Fig. 4(a). A difference spectrum of the metallized and annealed versus the clean surface exhibits negligible differences but shows absence of the V_{As} feature seen in Fig. 4(a). This latter difference is due to lower desorption temperature and thus higher As content of the (1×1) surface. Figures 4(a), 4(b), and 5 illustrate two major differences between the Au and Al metallizations: (i) a difference in deep level emission with reconstruction for Al but not for Au, and (ii) an increase in deep level emission with annealing for Au versus a decrease with annealing for Al. These spectral features are most evident for the most surface sensitive excitation conditions, e.g., 1 kV.

VI. DISCUSSION

The CLS results presented here demonstrate that deep levels are present within the GaAs band gap and that their emission intensity and spectral distribution vary with (100) surface preparation temperature, stoichiometry, and/or reconstruction. These spectral changes appear to be associated with changes in deep level density rather than any changes in recombination probability related to different band bending. Significant changes in band bending could cause large changes in NBG emission,[19] which are not evident for the spectra presented and compared. Furthermore, these deep levels are localized near the semiconductor surface or interface since the deep level emission increases monotonically with decreasing excitation energy. The additional emission at 0.7–1.2 eV for the As-rich (1×1) reconstruction may be associated with excess As, as reported previously.[22]

The interface deep levels are sensitive to the particular metal deposited. Au deposition induces new deep level emission which is similar for both low and high temperature reconstructions. This spectral insensitivity to local bonding and stoichiometry may be related to the disruptive nature of the Au–GaAs chemical interaction, which includes substantial interdiffusion.[4,5] The different spectral emission measured for Al deposition may also have a chemical origin. Al on the Ga-rich (4×2)-$c(8\times2)$ surface may be more effective in forming metal-anion bonds with any excess As than Al on the As-rich (1×1) surface. The higher emission at 0.8 eV for Al on the (1×1) surface shown in Figs. 4(b) and 5 is consistent with an excess As bonding environment (i.e., significant As–As versus Ga–As or Al–As coordination) as reported previously.[22] This higher emission intensity may in fact be centered at energies lower than 0.8 eV, since the low energy edge of CLS emission pictured in Fig. 4(b) may be the result of the Ge detector's response cutoff below 0.7 eV.

The spectral features displayed in Figs. 4 and 5 indicate that several discrete levels are present within the GaAs band gap at the Al–GaAs(100) interface whose relative density varies with surface preparation and interface annealing. Comparison of these spectra with those of Al on other reconstructions suggest characteristic emission energies of 0.8, 0.95, 1.05, and 1.2 eV, depending on the temperature, stoichiometry, and reconstruction.[24] Assuming that these energies correspond to optical transitions from the conduction band to deep levels in the band gap, one can attempt to associate particular features with previous observations. Thus the $\leqslant$0.8 eV feature can be associated with excess As at the interface,[23,25] while the 1.05 eV feature is usually attributed to a vacancy complex and appears related to substrate growth quality and/or damage.[26] The 0.95 eV transition was observed previously on both *n*- and *p*-type GaAs(100) and may account for E_F stabilization at Al/*p*-GaAs(100) interfaces.[24] It possibly corresponds to a transition from the conduction band to an As_{Ga} antisite defect level 0.52 eV above the valence-band maximum.[27] Overall, the results presented here underscore the role of surface and interface preparation in determining chemical composition and coordination and thereby discrete deep band gap levels which may play a role in Schottky barrier formation.

VII. CONCLUSIONS

Low energy cathodoluminescence spectroscopy measurements of As-rich, (1×1) and Ga-rich (4×2)-$c(8\times2)$ GaAs(100) surfaces reveal emission from discrete, deep level surface and metal interface states. Clean surfaces of the former exhibit additional emission in the 0.7–1.2 eV range. Au interfaces with both types of reconstructed surfaces exhibit additional midgap emission which increases further with annealing. Al interfaces exhibit deep level emission whose dominant spectral features change significantly with surface reconstruction and which are removed by interface annealing. These results emphasize the role of processing conditions in forming states which may contribute to the surface and interface electronic structure.

ACKNOWLEDGMENTS

The authors acknowledge partial support of this work by the Office of Naval Research (Grant No. N00014-91-C-0037). Soft x-ray photoemission spectra were obtained at the Synchrotron Radiation Center of the University of Wisconsin-Madison, which is supported by the National Science Foundation.

[1]W. Mönch, Rep. Prog. Phys. **53**, 221 (1990).
[2]E. H. Rhoderick and R. H. Williams, *Metal-Semiconductor Contacts*, 2nd ed. (Clarendon, Oxford, 1988).
[3]W. E. Spicer, Z. Lilienthal-Weber, E. Weber, N. Newman, T. Kendelewicz, R. Cao, C. McCants, P. Mahowald, K. Miyano, and I. Lindau, J. Vac. Sci. Technol. B **6**, 1245 (1988).
[4]J. H. Weaver, in *Analytical Techniques for Thin Films*, edited by K. N. Tu and R. Rosenberg, Treatise on Materials Science and Technology (Academic, New York, 1988), pp. 15–53.
[5]L. J. Brillson, Surf. Sci. Rep. **2**, 123 (1982); Comments Condens. Matter Phys. **14**, 311 (1989).
[6]L. Däweritz and R. Hey, Surf. Sci. **236**, 15 (1990).
[7]R. Z. Bachrach, R. S. Bauer, R. Chiaradia, and G. V. Hansson, J. Vac. Sci. Technol. B **3**, 1498 (1981).
[8]W. Mönch, in *Molecular Beam Epitaxy and Heterostructures*, NATO ASI Series (Martinuus Nijhoff, Dordrecht, 1985), Vol. 87, p. 331 and references therein.
[9]J. R. Arthur, Surf. Sci. **43**, 449 (1974).
[10]D. K. Biegelsen, R. D. Bringans, J. E. Northrup, and L.-E. Swartz, Phys. Rev. B **41**, 5701 (1990).
[11]M. D. Pashley, Phys. Rev. **40**, 10481 (1989).
[12]R. E. Viturro, J. L. Shaw, M. Mailhiot, L. J. Brillson, N. Tache, J. McKinley, G. Margaritondo, J. M. Woodall, P. D. Kirchner, G. D. Pettit, and S. L. Wright, Appl. Phys. Lett. **52**, 2052 (1988).
[13]L. J. Brillson, R. E. Viturro, J. L. Shaw, C. Mailhiot, N. Tache, J. McKinley, G. Margaritondo, J. M. Woodall, P. D. Kirchner, G. D. Pettit, and S. L. Wright, J. Vac. Technol. B **6**, 1397 (1988).
[14]D. Mao, A. Kahn, G. LeLay, M. Marsi, Y. Hwu, G. Margaritondo, M. Santos, M. Shayegan, L. T. Florez, and J. P. Harbison, J. Vac. Sci. Technol. B **9**, 2083 (1991).
[15]C. J. Spindt, M. Yamada, P. L. Meissner, K. E. Miyano, A. Herrera, W. E. Spicer, and A. J. Arko, J. Vac. Sci. Technol. B **9**, 2090 (1991).
[16]S. P. Wilks, J. I. Morris, D. A. Woolf, and R. H. Williams, J. Vac. Sci. Technol. B **9**, 2118 (1991).
[17]M. H. Hecht, Phys. Rev. B **41**, 7918 (1990).
[18]P. Skeath, C. Y. Su, I. Hino, I. Lindau, and W. E. Spicer, Appl. Phys. Lett. **39**, 349 (1981).
[19]L. J. Brillson, R. E. Viturro, J. L. Shaw, and H. W. Richter, J. Vac. Sci. Technol. A **6**, 1437 (1988).
[20]L. J. Brillson and R. E. Viturro, Scanning Electron Microsc. **2**, 789 (1988).
[21]M. D. Sturge, Phys. Rev. **127** 768 (1962).
[22]H. Birey and J. Sites, J. Appl. Phys. **51**, 619 (1980).
[23]R. E. Viturro, B. L. Olmsted, S. N. Haude-Walter, and G. W. Wicks, J. Vac. Sci. Technol. B **9**, 2244 (1991).
[24]I. M. Vitomirov, A. D. Raisanen, A. Finnefrock, R. E. Viturro, S. Chang, L. J. Brillson, P. D. Kirchner, G. D. Pettit, and J. M. Woodall (unpublished).
[25]R. E. Viturro, J. L. Shaw, and L. J. Brillson, J. Vac. Sci. Technol. B **6**, 1397 (1988).
[26]G. Dlubek, A. Dlubek, R. Krause, O. Brümer, K. Friedland, and R. Rentzsch, Phys. Status Solidi A **106**, 419 (1988).
[27]E. R. Weber, H. Ennen, U. Kaufmann, J. Windscheif, J. Schneider, and T. Wosinski, J. Appl. Phys. **53**, 6140 (1982).